



## PHotovoltaic Properties of Ultra-Small Copper Oxide Nanoparticles

**Ghada S. Mahdi**<sup>(1)</sup>  
Department of Physics,  
College of Science,  
Mustansiriyah University,  
Baghdad, Iraq.

**Randa K. Hussain**<sup>(2)</sup>  
Department of Physics,  
College of Science,  
Mustansiriyah University,  
Baghdad, Iraq

**Aseel M. Abdul Majeed**<sup>(3)</sup>  
Department of Physics,  
College of Science,  
Mustansiriyah University,  
Baghdad, Iraq

[ghada1997@uomustansiriyah.edu.iq](mailto:ghada1997@uomustansiriyah.edu.iq)   [dr.randa.kamel@uomustansiriyah.edu.iq](mailto:dr.randa.kamel@uomustansiriyah.edu.iq)   [aseelalaziz@uomustansiriyah.edu.iq](mailto:aseelalaziz@uomustansiriyah.edu.iq)

### Abstract:

Copper oxide (CuO) nanoparticles were synthesized chemically using aqueous copper nitrate by sol-gel method. The phase and structure investigations by XRD and SEM indicate to the spherical aggregation particles with an average particle size of 12 nm. The produced CuO nanoparticles showed an excellent purity, as confirmed by EDX measurement. The optical properties of Uv-Vis spectroscopy displayed a highly absorption band in range of 200 nm -350 nm of a bandgap 3.5 eV. These results support the preparation of these nanostructures for solar cell applications. The heterojunction (Ag/CuO/Si/Ag) characterized in term of current-voltage properties of as a solar cell. It displayed a filling factor (F.F) and a power conversion efficiency ( $\eta$ ) were 48.05% and 0.105% respectively.

**Keywords:** Nanoparticles, Copper Oxide, Optical properties, Solar cell, heterojunction, Structural properties

### Introduction:

Our lifestyles require renewable, sustainable, and clean energy sources that keep pace with scientific and technological advancements. Solar cells assumed from the best options for obtaining energy under these conditions. However, a number of obstacles have significantly impacted the widespread use and application of solar cells, such as the efficiency of converting solar energy into electricity, the stability of efficiency, and, to some extent, the cost [1-2]. Nanomaterials represent an alternative option for obtaining solar cells with better efficiency and lower costs by relying on the development paths of nanomaterials, especially metal oxides.

Metal oxide at nano scale nanostructures had intrigued researchers because of their characteristics, that fluctuate according to size and form, and can be synthesized through several methods [3]. Their elevated surface to - volume ratio renders them exemplary applicant for diverse sensing fields [4- 5], photocatalysis [6], solar cells [7-8], electronics [9-11]. Stability solar cell represents the essential for meeting addressing upcoming times non- depletion energy requirements, rendering it essential to choose economical materials such as metal oxides [12]. A solar cell is an electronic apparatus transforms the optical energy from sun to an electrical energy. At sunlight impinges upon the solar cell, will produces electricity and voltage [13, 14]. The operation of a solar cell can be summarized in two basic

steps: absorption of sunlight, which raises the energy levels of electrons, followed by the migration of electrons to higher energy levels and their transfer to the external circuit. After these electrons discharge their energy, they return to the solar cell. Copper oxide (CuO) particles are of significant interest as nanoscale conductors due to their advantageous properties, including abundance, elevated optical absorption coefficient, low energy range, and non-toxicity [15-16]. It is a semiconductor matter extensively utilized in energy photovoltaic conversion manufacturing owing to its superior optical absorption and non-toxic properties leading to reduced production expenses. It is a p-type semiconductor have a band gap varies between 1.2 eV – 3.35 2.0 eV in nanoscale influenced by size of the nanoparticle, while the bulk CuO possess an energy band gap about 1.2 eV [17-19]. Hence, the peak absorption of the light spectrum is expected to be in the ultraviolet - visible band, which makes it suitable for solar cell applications [9,20].

This feature makes copper oxide unique in is a significant substance utilized in solar energy conversion [21], besides of other varied physical and chemical properties, which depend on the morphology of nanostructures [22,23]. Numerous technologies and techniques facilitate the preparation of CuO nanopowder. The present paper describes a simply production of copper oxide nanoparticles using aqueous copper oxide nitrate and its future applications in solar cells and study optical and structure properties of nano material. The influence of the preparation method on the crystal size of particles and their relationship to the optical properties is investigated.

### Methods and materials

In this study, a chemical method was adopted to prepare copper oxide nanoparticles from Nitrous copper nitrate with the chemical formula  $Cu(NO_3)_2 \cdot H_2O$  Salt of 0.2 gram of  $Cu(NO_3)_2$  was dissolved in 20 mL volume of distilled water and stirred until the salt was completely dissolved, forming a blue solution of molarity 0.04 M. Another sodium hydroxide NaOH solution was prepared by dissolved 0.1 gram in 25 ml volume of distilled water and mixed well for 5 minutes. The sodium hydroxide solution was added to the blue solution by a slow drip method, continuing for 10 minutes with continuous stirring to ensure complete mixing. The solution was then left to resolve for several minutes. It was washed thoroughly twice with water and once with ethanol and left to dry on a hot plate until it turned black, as shown in Figure 1. The black powder was collected with a spoon, ground, and dried at  $400^\circ C$  for two hours to form pure copper oxide.



Figure (1): Nanoparticle solution after distillation

Fabrication of copper oxide nanoparticles based as solar cell set up was done by deposited a thin film of CuO NPs on a silicon (Si) substrate to form an active layer for solar cell to manufacture the heterojunction (Ag/CuO/Si/Ag). CuO NPs was deposited on the silicon substrate ( $1 \times 1 \text{ cm}^2$ ) by drop-casting technique, the deposited layer diameter 0.75 cm. The silicon surface was treated with HF to create surface roughness, which enhances the adhesion of subsequent layers. This CuO layer acts as an efficient light absorber was deposited by drop casting method on a heat plate to get uniform film. After annealing to improve crystallinity and adhesion, a metal electrode of silver is deposited on top of the CuO layer using silver paste. This top electrode serves as the current collector. The careful alignment and deposition of these electrodes are crucial for achieving good electrical contact and high device performance. Figure (2) displays the final setup of solar cell.

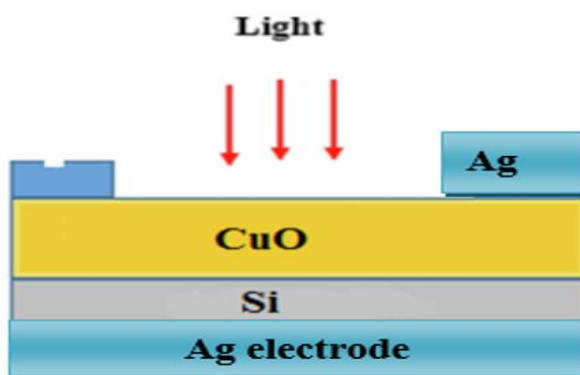


Figure (2): Schematic diagram of the prepared solar cell.

## Results and Discussion

### 3-1 XRD analyses

X-ray diffraction of the CuO NPs produced by chemical preparation showed the crystalline structure, phase and high purity within the nanoscale. The figure (3) illustrated the diffraction pattern for the angle  $2\theta$  range from  $30^\circ - 80^\circ$ , the peaks appeared at  $35.553^\circ$  and  $38.730^\circ$  recording to Miller indices  $(1\bar{1}1)$ ,  $(111)$ , respectively. This was verified by comparing with the ASTM card no. 050661.

The widen of typical peaks was proved the nano scaled particles formation, exhibited a successful preparation of CuO NPs. The CuO nanocrystals size determined by Debye-Scherrer's formula [24].

$$D (A^\circ) = k\lambda/\beta\cos\theta \text{ ----- (1)}$$

Where, D remarked to the crystallite size, k is Scherrer's constant (typically valued at 0.9), while, the wavelength of X-ray wavelength is represented by  $\lambda$  denotes the (1.540 Å), the symbol of  $\beta$  stands for the full width at half maximum (FWHM) of the diffraction peaks measured at the Bragg angle  $\theta$ . The Copper oxide nanoparticles were formed in a crystallite its average size was 12nm. Table (1) summarized the structure parameters, the dislocation density ( $\delta$ ) and microstrain ( $\epsilon$ ) were calculated by formula (2) and (3) respectively [24]:

$$\delta = \frac{1}{D^2} \text{..... (2)}$$

$$\epsilon = \frac{\beta}{4\tan(\theta)} \text{..... (3)}$$

The crystallite size of the two principle peaks shows small values which confirm that the material is nanocrystalline in nature. A crystallite size below 100 nm indicates that the sample likely contains fine grains or nanoparticles. While the slightly larger crystallite size in peak ( $2\theta=38.825$ ) suggests that region might be more ordered or less affected by strain. The table (1) indicated that the amount of defects or dislocations per unit area in the crystal is high means more imperfections, which can impact electrical properties. Values fall in the typical range for nanomaterials and support the microstrain findings. The lattice distortions or internal strain within the crystal structure arises from defects, dislocations, grain boundaries, or residual stresses. The relatively high values here indicate that the material experiences noticeable internal stress, which is common in nanostructured chemically synthesized materials.

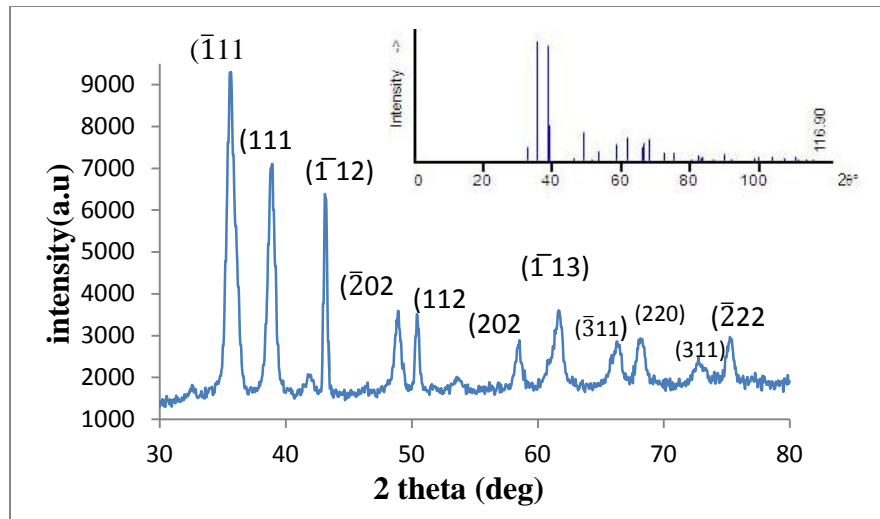


Figure (3): XRD pattern for CuO NP

Table (1): Structural parameters of CuO NPs

2θ (Deg.)	FWHM (Deg.)	d <sub>hkl</sub> Exp.(Å)	Miller Indices	Phase	D (nm)	Average D(nm)	Dislocation density (cm <sup>-2</sup> )	Microstrain
35.63	0.8	2.521	( $\bar{1}11$ )	Monoclinic	10	12	$9.19 \times 10^{11}$	$1.09 \times 10^{-2}$
38.825	0.634	2.317	(111)	Monoclinic	13		$5.76 \times 10^{11}$	$7.85 \times 10^{-3}$

The data obtained by XRD analyzed by Williamson –Hall method plot, for  $\beta$ -instrument of 0.3 the W-H plot showing a high scattering of points ( $R^2 = 0.1272$ ) around the linear fitting, as illustrated in Figure(4). The microstrain ( $\epsilon$ ) and crystal size (D) are  $7.464 \times 10^{-3}$  and 37.45 nm respectively. The microstrain confirmed good agreement with the Scherrer's method, but the size witnessed a large difference, which may be due to overlapping peaks or noise as seen in inset picture in Figure (3), a crowded peaks around angle  $40^\circ$  and  $60^\circ$ .

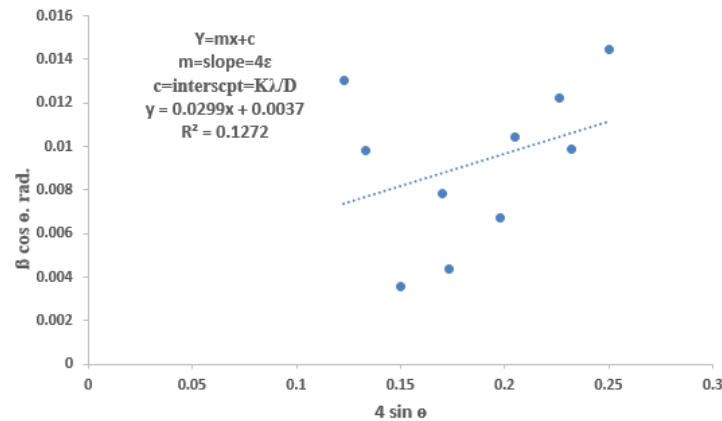


Figure (4): Wallison-Hall plot

### 3-2 SEM analyses

SEM analysis was applied to investigate the surface morphology of the chemically synthesized CuO NPs. Figure (5-a, -b and -c) expose to view the CuO NPs SEM images in 200 nm scale, enlarged to 10 μm and particle-size histogram as in order. As it noticed, CuO nanostructure own a small-sized layered sheets shape of thickness around 25 nm, poor homogeneity with a jagged surface due to the small particles of high surface tension energy, which accumulate the particles together and complete particles separation cannot have obtained (see Figure 5-b). However, particles aggregated were remarked, this may due to high NaOH content, the study [25] indicated the effect of the amount of sodium hydroxide on the size and agglomeration of particles. Exceeding NaOH may producing highly agglomerated particles, and the size of the particles changes. The appearance of larger grains and nanoparticle aggregation is likely due to the high surface area and elevated surface energy characteristic of the CuO nanoparticles [26]. The particle size distribution confirms the low – scale size, the most particle size is in the range below 10 nm giving it a Gaussian form. As a reason of their high surface area-to-volume ratio, the nanoparticles tended to stick together or form agglomerates as a result of attractive physical interactions.

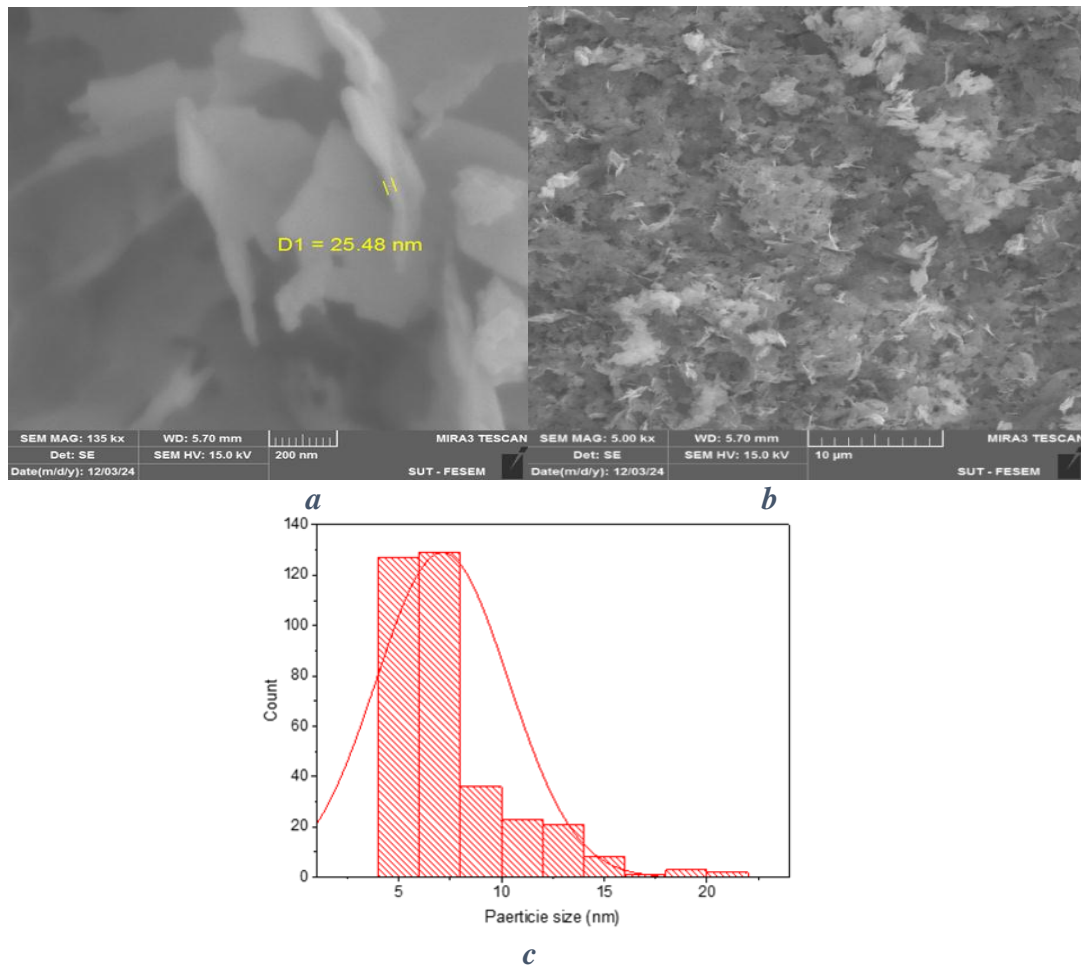


Figure (5): SEM images of CuO NPs

### 3-3 EDX analyses

Energy Dispersive X-ray Spectroscopy (EDX) examination proved the chemical configuration of the synthesized CuO nanostructure. The Figure (6) shows the spectrum of the X-ray diffraction, and the peaks in it are limited to the presence of peaks specific to the elements copper (Cu) and oxygen (O), which proves the purity of the prepared CuO nanoparticles and their freedom from impurities. From the weight % and atomic % percentages of the chemical elements that are given in the inset table, it revealed the presence of copper (Cu) and oxygen (O) as the main components, with their weight percentages reaching 60% and 40%, respectively, while the atomic percentages of copper and oxygen were 27.4% and 72.6%, respectively. The (Au) element peaks attributed to the presence of the Au element

that appeared in multiple peaks is due to the gold coating layer during the examination. These results are consistent with the predicted chemical composition of copper oxide (CuO) and reflect the good purity of the sample. On the other hand, X-ray diffraction (XRD) analysis confirmed the monoclinic crystal structure of copper oxide, with diffraction peaks matching the standard data from the JCPDS card no. 050661 for CuO which exhibits good thermal and chemical stability in contrast to other cuprous of higher oxidation number. This agreement between the EDX and XRD results clearly demonstrates the successful preparation of the material, both in terms of chemical composition and crystal structure, enhancing the reliability of the sample for functional applications in the electronic or optical fields [17, 27].

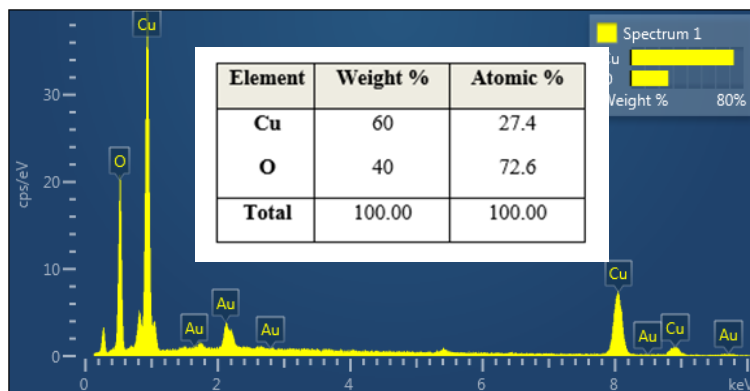


Figure (6): EDX spectra of the CuO nanoparticles

### 3-4 Optical properties

The UV-Vis Spectroscopy was used to investigate the optical behavior of copper oxide nanostructures prepared by chemical method. The optical properties were studied through absorption spectrum and energy gap. The UV-Vis absorption spectra of CuO NPs exhibited a broad absorption peak within the wavelength range of 200 nm to 350 nm, as depicted in Figure (7). The absorption edge reaches around short wavelengths resulting in increased of the optical band gap energy ( $E_g$ ). Very small crystallites (10–13 nm) result in a larger surface area, which can enhance light absorption. As the dimensions decreased (the case in ultra-small size in nanoparticles) the continues energy levels in bulk were split into quantized discreet levels causing a widening in band gap. This indicates that a smaller nanoparticles absorb and emit higher-energy (shorter wavelength). The improved absorbance resulting from the large surface area combined with the availability of

effective sites for light interaction with the material may provide an opportunity to improve the performance of solar cells. The optical band gap energy is calculated from experimental absorbance. Planck's law, as given in Eq. (4) [28], was applied for calculation the bandgap energy directly from  $\lambda_{cut}$ :

$$E_g = hc/\lambda_{cut} = 1240/\lambda_{cut} \dots\dots\dots(4)$$

where  $E_g$  is the energy gap,  $h$  is Planck's constant ( $h=6.626 \times 10^{-34}$  J.s),  $c$  is the light velocity ( $3 \times 10^8$  m/s), and  $\lambda$  is the wavelength.

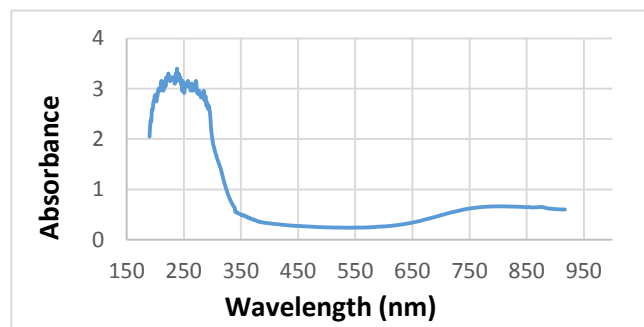


**Figure (7): UV-Vis spectrum of CuO nanoparticles**

absorption coefficients can be determined graphically by Tauc's relationship as in equation (5) [26]:

$$(\alpha h\nu)^r = A(h\nu - E_g) \dots\dots\dots(5)$$

Where  $\alpha$  remarked to the absorption coefficient, while  $\nu$  refers to the photon frequency,  $A$  is a constant ( $A= 0.9$ ), and  $r$  is a value of the direct transition ( $r = 2$ ). The common approach to determine the band gap the don by plotting the curve between  $(\alpha h\nu)^r$  and photon energy ( $h\nu$ ) on x-axis. By intercept of the tangent of the linear portion curve, crosses the x- axis obtained the band gap value. The band gap energy was 3.5 eV, which is less than that reported in the literature [18, 29], see Figure (8).

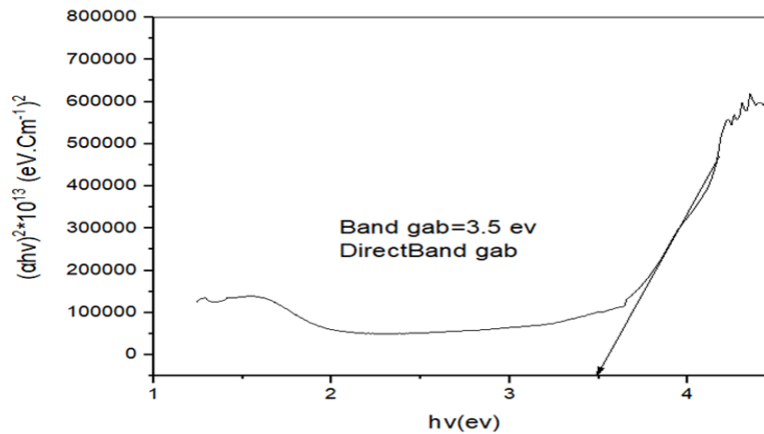


**Figure (8): Optical energy band gap of CuO NPs**

The solar cell (Ag/CuO/Si/Ag) heterojunction was investigated by the current–voltage properties. It was found that the forward bias current exceeds the reverse bias current, as illustrated in Figure 9a. As the forward voltage is below 3 volts, an electric current is produced due to the re-combination process of electron-hole pairs. Although, higher voltages enable the electrons to gain sufficient energy for crossing the junction’s potential barrier. The resulting current is referred to as the diffusion current. Figure 9b presents the reverse current–voltage behavior and the heterojunction properties recorded at both dark conditions and at under light of tungsten lamp of 1000mW / cm<sup>2</sup> illumination power.

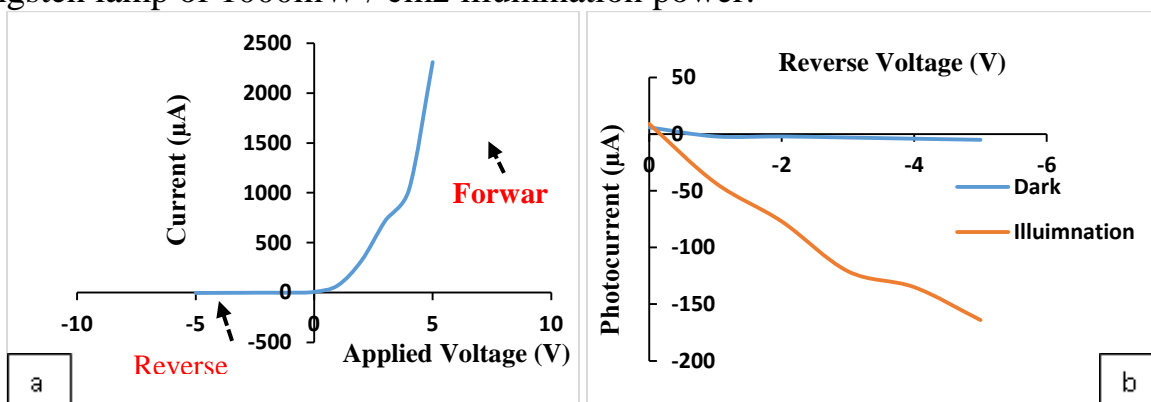


**Figure (9): Current-Voltage properties: (a) in forward and reverse biasing, (b) dark and lightening**

The reverse current of the (Ag/CuO/Si/Ag) heterojunction under illumination is noticeably higher in contrast in dark conditions, referring to the photo-generated charge carriers subscribe significantly to the photocurrent through electron-hole pair generation. This behavior offers valuable insight into the formation of electron-hole pairs as a result of incident photon energy. The major photovoltaic parameters containing the open-circuit voltage ( $V_{oc}$ ), short-circuit current ( $I_{sc}$ ), fill factor (FF), and conversion efficiency—are measured and analyzed as given by Figure 10, which presents the I–V characteristics under illumination with varying load resistances. This experimental approach provides a straightforward method

for evaluating the efficiency of a solar cell. To determine efficiency, two key points must be considered: the short-circuit current ( $I_{sc}$ ), which occurs when the load resistance ( $R$ ) and voltage ( $V$ ) are both zero, and the open-circuit voltage ( $V_{oc}$ ), which is observed when the load resistance is high enough to reduce the net current to zero. These findings reinforce the effectiveness of the CuO-based heterojunction structure in enhancing photoresponse and serve as a foundation for optimizing future solar cell designs based on similar configurations. It could specify the maximum power rectangle by Equation (6) to obtain the maximum solar energy efficiency, Figure (10) shows the open – circuit (current-voltage) characteristics for CuO/Si heterojunction. Short- circuit current( $I_{sc}$ ), open –circuit voltage( $V_{oc}$ ), Efficiency ( $\eta$ ) and fill factor (F.F) and have been measured using equations (6) and (7) [30] respectively, were the obtain results of 15  $\mu$ A, 154 mV, 48.05% and 0.105 % respectively. All the results relieve that the heterojunction CuO/Si could be used for solar cell applications [31,32].

$$\eta = \frac{P_m}{P_{in}} = \frac{V_m I_m}{P_{in}} * 100\% \quad \text{--- (6)}$$

$$FF = \frac{V_m I_m}{V_{oc} I_{sc}} \quad \text{--- (7)}$$

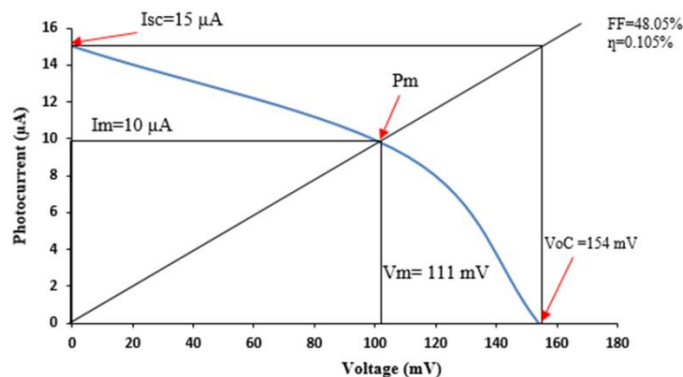


**Figure (10): Photocurrent- voltage of the (Ag/CuO/Si/Ag) solar cell**

These results are somewhat acceptable when compared to previously published results in [33-34] for CuO without additions or improvements, their efficiency were 0.64% and 0.0863% respectively. The reasons that affected the efficiency and

filling factor can be explained based on the resulting structural properties. The small crystal size causes an increase in defects, which appear in the form of dislocation defects, causing charge losing. Furthermore, increased microstrain may lead to increased recombination. Very small crystal size resulted more grain boundaries, which act as recombination centers. These boundaries can trap carriers, preventing them from reaching the electrodes. Nanocrystals have too many grain boundaries hurt charge transport and reduce efficiency. High dislocation density indicates many structural defects. These defects create non-radiative recombination centers, and lower open-circuit voltage ( $V_{oc}$ ) and fill factor (FF). High dislocation density leads to exceeds recombination and decreasing power conversion efficiency. The high lattice distortions create trap states (defect levels within the band gap). Trap states will be raising recombination of electrons and holes, decreased carrier lifetime. And lower short-circuit current ( $I_{sc}$ ) and total efficiency. High microstrain tends to reduce efficiency by increasing charge losses. The calculated band alignment of the p-CuO / n-Si heterojunction reveals important interfacial properties. The electron affinities of CuO (4.07 eV) and Si (4.05 eV) [35] are nearly identical, resulting in a very small conduction band offset ( $\Delta E_c = 0.02$  eV). This facilitates efficient electron transfer across the junction. In contrast, the valence band offset is large ( $\Delta E_v = 2.40$  eV), creating a substantial barrier for hole transport from Si into CuO. The wide band gap of nanostructured CuO ( $E_g =$

3.5 eV) makes it a suitable light-absorbing and hole-blocking layer, while the narrower band gap of Si ( $E_g = 1.12\text{eV}$ ) supports electron conduction. Upon contact, Fermi level equilibration induces band bending and depletion region formation, which assist in charge separation. Overall, the CuO/Si heterojunction exhibits favorable band alignment for photovoltaic and photodetector applications, as the low  $\Delta E_c$  promotes electron transport while the high  $\Delta E_v$  suppresses recombination, Figure (11) shows the bending band energy diagram of p-CuO / n-Si heterojunction.

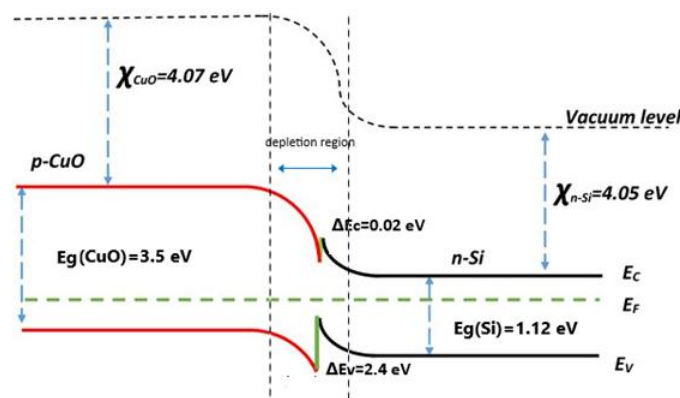


Figure (11): Heterojunction band diagram

## Conclusion

The copper oxide NPs were achievement synthesized adopting the chemical method. Velocity, cost-effectiveness, and ecological sustainability in comparison to alternative. Copper oxide NPs of a monoclinic structure with small average particle size (12 nm) were effectively fully prepared exhibiting high absorption in region 200 nm to 350 nm possessing an energy band gap of 3.5 eV. The ultra-small size has a crucial role in increasing the absorption. The heterojunction Ag/CuO/Si/Ag fabricated as solar cell achieved a filling factor and efficiency of (48.87% and 0.105%). These are acceptable results when compared with the other solar cells fabricated from modified metal oxides. The possibility of increasing efficiency by improving the p-n interface may have suggested as future work.



## References

1. Abdelrahman O. Ali, Abdelrahman T. Elgohr , Mostafa H. El-Mahdy, Hossam M. Zohir, Ahmed Z. Emam, Mostafa G. Mostafa, Muna Al-Razgan, Hossam M. Kasem, Mohamed S. Elhadidy, Advancements in photovoltaic technology: A comprehensive review of recent advances and future prospects ,Energy Conversion and Management: X, Volume 26, April 2025, 100952
2. Val Hyginus Udoka Eze, Kiiza Richard, Kelechi John Ukagwu, Wisdom Okafor, Factors Influencing the Efficiency of Solar Energy Systems, Journal of Engineering, Technology & Applied Science, Volume. 6 | Issue. 3 | 119-131(2024)
3. J. Asenjo-Castillo, I. Vargas-Blanco, Espectroscopia De Plasmas en condiciones de presión atmosférica. Rev. Tecnol en Marcha. 29(6), 47 (2016). <https://doi.org/10.18845/tm.v29i6.2901>
4. B. Renganathan ,C.K. Gopakumar ,A. Kalai Priya ,Subha Krishna Rao, D. Sastikumar, M. Silambarasan, Nagarajan Kannapiran, Optimizing Gas Sensing Performance of CuO Nanoparticles via Sol-Gel Synthesis Approach for Efficient Detection of Ammonia Gas, Materials Research Bulletin Volume 170, 2024, 112556.
5. Lalitha Ammadu Kolahalam , K.R.S. Prasad ,P. Murali Krishna ,N. Supraja ,S. Shanmugan, The exploration of bio-inspired copper oxide nanoparticles: synthesis, characterization and in-vitro biological investigations, Heliyon 8 (2022) e09726.
6. K.A. Aadim, Detection of laser-produced tin plasma emission lines in atmospheric environment by optical emission spectroscopy technique, Photonic Sensors. Iraqi J. Phys. 7(4), 289–293 (2017). <https://doi.org/10.1007/s13320-017-0429-x>
7. Mohammed J. Mohammed Alia, Munthir Mohammed Radhyb, Salam Jumah mashkoor, Ehab M. Alib, Synthesis and characterization of copper oxide nanoparticles and their application for solar cell, Materials Today Processing, Volume 60, Part 2, 2022, Pages 917-921
8. M.H. Oudah, M.H. Hasan, A.N. Abd, Synthesis of copper oxide thin films by electrolysis method based on Porous Silicon for Solar Cell Applications, IOP Conf. Ser. Mater. Sci. Eng. (2020).
9. Ahed M. Al-Fa'ouri ,Omar A. Lafi ,Husam H. Abu-Safe ,Mahmoud Abu-Kharma, Investigation of optical and electrical properties of copper oxide - polyvinyl alcohol nanocomposites for solar cell applications, Arabian Journal of Chemistry, Volume 16, Issue 4, April 2023, 104535.
10. Growth and characterization of Cu<sub>2</sub>O films made by rapid thermal oxidation technique Chinese Physics Letters Open source preview, 2005, 22(11), pp. 2977–2979.
11. Aseel Mustafa Abdul Majeed, Itab F. Hussein, Rana O. Abd-Jalil, Fabrication of High Responsivity for MgO NPs/PSi Heterojunction Device by Sol-Gel Technique, Silicon, 12(5), pp. 1007–1010, (2020).
12. Ali Hameed Rasheed, Anfal Ismael Ibrahim, Suraa Reaad, Mustafa M. Kadhim, Synthesis and Characterization of CuO Nanoparticles For Increase The Efficiency of the photovoltaic cell, Egypt. J. Chem. Vol. 66, No. 1 pp. 49 - 53 (2023).



13. S. Chandra, Textbook of plasma physics, 1ed. India (2010)
14. J. Asenjo-Castillo, I. Vargas-Blanco, Espectroscopia De Plasmas en condiciones de presión atmosférica. Rev. Tecnol en Marcha. 29(6), 47 (2016). <https://doi.org/10.18845/tm.v29i6.2901>
15. Xing, C., Lei, Y., Liu, M., Wu, S., He, W., & Zheng, Z. (2021). Environment friendly Cu-based thin film solar cells: materials, devices and charge carrier dynamics. Physical Chemistry Chemical Physics, 23(31), 16469-16487.
16. P.C. Okoye , S.O. Azi , T.F. Qahtan , T.O. Owolabi , T.A. Saleh, Synthesis, properties, and applications of doped and undoped CuO and Cu<sub>2</sub>O nanomaterials, Materials Today Chemistry, Volume 30, 101513, 2023
17. Bahaa Hassoun Abbas, Nisreen Kh Abdalameer, Raghad S. Mohammed, Synthesis of Copper Oxide Nanostructures by Ar Plasma Jet and Study of Their Structural and Optical Properties, Iraqi Journal of Science, 2024, Vol. 65, No.4.
18. R. S. Mohammed, K. A. Aadim, Kh. A. Ahmed, " Synthesis of CuO/ZnO and MgO/ZnO Core/Shell Nanoparticles with Plasma Jets and Study of their Structural and Optical Properties," Karbala International Journal of Modern Science, vol. 8, pp. 213-222, 2022
19. P. Vinothkumar, Chellasamy Manoharan, Chellasamy Manohar and B. Shanmugapriya Mohammed Bououdina, Effect of reaction time on structural, morphological, optical and photocatalytic properties of copper oxide (CuO) nanostructures, Journal of Materials Science: Materials in Electronics 30(6):1-14(2019).
20. Raid A. Ismail, Aseel Mustafa Abdul, Preparation and investigation of nanostructured SnO<sub>2</sub>:Pd/ porous silicon/c-Si heterostructure solar cell, Journal of Solid State Electrochemistry, 25(3), pp. 1039–1048, (2021).
21. Safana alzalzala and Amer M. J. AL-Shamari, Preparation and Characterization of Copper Oxide CuO (II) nanoparticles Prepared by a Hydrothermal Method and for Solar Cells applications, Journal of Kufa-Physics, Vol. 15 No. 02 (2023).
22. Qiu S, Zhou H, Shen Z, Hao L, Chen H, Zhou X. Synthesis, characterization, and comparison of antibacterial effects and elucidating the mechanism of ZnO, CuO and CuZnO nanoparticles supported on mesoporous silica SBA-3. RSC Adv. 2020;10(5):2767–85.
23. Carmen Gherasim ,Petronela Pascariu ,Mihai Asandulesa ,Marius Dobromir, Florica Doroftei ,Nicusor Fifere, Andrei Dascalu , Anton Airinei, Copper oxide nanostructures: Preparation, structural, dielectric and catalytic properties, Ceramics International, Volume 48, Issue 17, 1 September 2022, Pages 25556-25568.
24. Feng Xu, Yong-Cheng Shi, Donghai Wang, X-ray scattering studies of lignocellulosic biomass: A review, Carbohydrate Polymers, Volume 94, Issue 2, 15 May 2013, Pages 904-917.
25. Khuram Ali, Muhammad Sajid, Suriani Abu Bakar, Ayesha Younus, Hassan Ali, Muhammad Zahid Rashid, Synthesis of copper oxide (CuO) via coprecipitation method: Tailoring structural and optical properties of CuO nanoparticles for optoelectronic device applications, Hybrid Advances, Volume 6, August 2024, 100250.



26. Abdulla, H.A., Mohammed, N.J., Abdul Majeed, A.M., Impact of substrate -target distance on the hemispherical expansion plume generated by the deposit of SnSe nanoparticle thin films, Kuwait Journal of Science, Volume 50, Issue 2, Pages 174 - 181 April (2023).
27. Randa Kamel Hussain, Yahya M Abdul-Hussein, Aqel Mashot Jafar, Mohammed K. Khalaf, Structural, Optical, and Electrical Properties of SrTiO<sub>3</sub>: La Thin Films Using AACVD Technique, AIP Conference Proceedings, 2023.
28. Radhakrishnan, A.A. and Beena, B.B. (2014) Structural and Optical Absorption Analysis of CuO Nanoparticles. Indian Journal of Advances in Chemical Science, 2, 158-161.
29. Mohd Shkir, Farhat S. Khan ,Thamra Alshahrani, Biosynthesis of CuO nanoparticles using Caralluma adscendens leaf extract for developed antibacterial and photocatalytic dye degradation properties, Materials Chemistry and Physics, Volume 344, 2025, 131118.
30. Abdelghani Rahal, Idris Bouchama, M. A. Ghebouli, B. Ghebouli, d M. Fatmi, S. Alomairy, S. Boudour, F. Benlakhdar and M. Chellouche, Optimization of structural and electronic properties in CuO/CIGS hybrid solar cells for high efficiency, sustainable energy conversion, RSC Adv., 2025, 15, 23311–23318.
31. Karthigaimuthu Dharmalingam, Arjun Kumar Bojarajan, Ramalingam Gopal, Elangovan Thangavel, Salah Addin Burhan Al Omari & Sambasivam Sangaraju, Direct Z-scheme heterojunction impregnated MoS<sub>2</sub>–NiO–CuO nanohybrid for efficient photocatalyst and dye-sensitized solar cell, Scientific Reports volume 14, Article number: 14518 (2024).
32. Aseel Mustafa Abdul Majeed, Asmaa Deiaa Nusseif, Nibras salah Hamed, Investigations of ZnO-NiO/Psi heterojunction for solar cell application, AIP Conference Proceedingsthis link is disabled, 2144, 030015 ,( 2019).
33. Terence K S Wong,, Siarhei Zhuk, Saeid Masudy-Panah, Goutam K Dalapati , Current Status and Future Prospects of Copper Oxide Heterojunction Solar Cells, Materials (Basel). 2016 Apr 7;9(4):271. doi: 10.3390/ma9040271
34. Thi Ha Tran, Viet Tuyen Nguyen , Copper Oxide Nanomaterials Prepared by Solution Methods, Some Properties, and Potential Applications: A Brief Review, Int Sch Res Notices. (2014) 16:856592.
35. Amir Hussain, Heisnam Shanjit Singh &Atowar Rahman ,Electrical characteristics of (n)Si/(p)PbS heterojunction prepared by chemical bath deposition technique, Superlattices and Microstructures, 89 (2016) 43-52.

## الخصائص الكهروضوئية لجسيمات أكسيد النحاس فائقة التوصيل

غادة صباح مهدي (2)

رندة كامل حسين (2)

أسيل مصطفى عبد المجيد (3)

قسم الفيزياء، كلية العلوم،  
الجامعة المستنصرية، بغداد، العراق

قسم الفيزياء، كلية العلوم،  
الجامعة المستنصرية، بغداد، العراق

قسم الفيزياء، كلية العلوم،  
الجامعة المستنصرية، بغداد، العراق

[ghada1997@uomustansiriyah.edu.iq](mailto:ghada1997@uomustansiriyah.edu.iq)

[dr.randa.kamel@uomustansiriyah.edu.iq](mailto:dr.randa.kamel@uomustansiriyah.edu.iq)

[aseelalaziz@uomustansiriyah.edu.iq](mailto:aseelalaziz@uomustansiriyah.edu.iq)

### مستخلص البحث:

تم تصنيع جسيمات أكسيد النحاس النانوية (CuO) كيميائياً باستخدام نترات النحاس المائية. أشارت فحوصات الطور والبنية بواسطة حيود الأشعة السينية والمجهر الإلكتروني الماسح إلى جسيمات تجميع كروية بمتوسط حجم جسيم يبلغ 12 نانومتر. أظهرت جسيمات أكسيد النحاس النانوية الناتجة نقاءً ممتازاً، كما أكدته قياس EDX. أظهرت الخصائص البصرية لتحليل الطيف فوق البنفسجي-المرئي نطاق امتصاص عالي في نطاق 200 نانومتر -350 نانومتر من فجوة نطاق 3.5 إلكترون فولت. تدعم هذه النتائج تحضير هذه البنى النانوية لتطبيقات الخلايا الشمسية. يتميز الوصلة غير المتجانسة (Ag/CuO/Si/Ag) من حيث خصائص التيار والجهد كخلية شمسية. أظهر عامل ملء (F.F) وكفاءة تحويل الطاقة (% 48.05 n) و0.105% على التوالي.

**الكلمات المفتاحية:** الجسيمات النانوية، أكسيد النحاس، الخصائص البصرية، الخلية الشمسية، الوصلة غير المتجانسة، الخصائص الهيكلية.

ملاحظة: هل البحث مستل من رسالة ماجستير او اطروحة دكتوراه؟ نعم : مستل من رسالة ماجستير